

Dynamic approach to description of entrance channel effects in angular distributions of fission fragments

D. O. Eremenko,^{1,2,*} V. A. Drozdov,¹ O. V. Fotina,^{1,2} S. Yu. Platonov,^{1,2} and O. A. Yuminov¹
¹*Skobeltsyn Institute of Nuclear Physics, M.V. Lomonosov Moscow State University, Moscow 119991, Russia*
²*Faculty of Physics, M.V. Lomonosov Moscow State University, Moscow 119991, Russia*
 (Received 10 January 2016; revised manuscript received 24 May 2016; published 5 July 2016)

Background: It is well known that the anomalous behavior of angular anisotropies of fission fragments at sub- and near-barrier energies is associated with a memory of conditions in the entrance channel of the heavy-ion reactions, particularly, deformations and spins of colliding nuclei that determine the initial distributions for the components of the total angular momentum over the symmetry axis of the fissioning system and the beam axis.

Purpose: We develop a new dynamic approach, which allows the description of the memory effects in the fission fragment angular distributions and provides new information on fusion and fission dynamics.

Methods: The approach is based on the dynamic model of the fission fragment angular distributions which takes into account stochastic aspects of nuclear fission and thermal fluctuations for the tilting mode that is characterized by the projection of the total angular momentum onto the symmetry axis of the fissioning system. Another base of our approach is the quantum mechanical method to calculate the initial distributions over the components of the total angular momentum of the nuclear system immediately following complete fusion.

Results: A method is suggested for calculating the initial distributions of the total angular momentum projection onto the symmetry axis for the nuclear systems formed in the reactions of complete fusion of deformed nuclei with spins. The angular distributions of fission fragments for the $^{16}\text{O} + ^{232}\text{Th}$, $^{12}\text{C} + ^{235,236,238}\text{U}$, and $^{13}\text{C} + ^{235}\text{U}$ reactions have been analyzed within the dynamic approach over a range of sub- and above-barrier energies. The analysis allowed us to determine the relaxation time for the tilting mode and the fraction of fission events occurring in times not larger than the relaxation time for the tilting mode.

Conclusions: It is shown that the memory effects play an important role in the formation of the angular distributions of fission fragments for the reactions induced by heavy ions. The approach developed for analysis of the effects is a suitable tool to get insight into the complete fusion-fission dynamics, in particular, to investigate the mechanism of the complete fusion and fission time scale.

DOI: [10.1103/PhysRevC.94.014602](https://doi.org/10.1103/PhysRevC.94.014602)

I. INTRODUCTION

The investigation of angular distributions of fission fragments (ADs) for heavy-ion-induced reactions has brought out many interesting possibilities to gain new information on fusion and fission dynamics [1–4]. In particular, it was shown in Refs. [5–7] that ADs depend on the durations of different stages of heavy-ion-induced fission and their analysis makes it possible to obtain information about fission time scale and nuclear dissipation. It is well known [1] that consideration of the dynamic aspects of fusion is important to explain the behavior of the anisotropy of angular distributions of fission fragments (ADA) at subbarrier energies, namely, its anomalously high values with respect to the predictions of the standard transition-state model [2,8] for some reactions with heavy ions. The first attempts to explain the anomalously high ADA have been taken within the preequilibrium K -state model [9,10] and the quasifission orientation-dependent model of Refs. [11,12]. In both models, a significant role is played by the conditions that are realized in reaction entrance channels. The pre-equilibrium K -states model predicts ADA significantly higher than that of the standard transition-state model [8] for near- and subbarrier reactions with entrance channel mass

asymmetries larger than the Businaro-Gallone critical mass asymmetry $[(A_t - A_p)/(A_t + A_p) = 0.90]$, where A_t and A_p are the mass numbers of the incident and target nuclei]. The quasifission orientation-dependent model asserts that for collision of projectiles and actinide nuclei there is a critical angle orientation of the prolate deformed nucleus of the target relative to the beam. For the angles less than this critical value, a dinuclear system is formed and then decays quickly (quasifission) with the anomalously high ADA.

It was later demonstrated in Refs. [5,13–15] that ADA is strongly dependent on the individual features of colliding nuclei (such as spin and deformation) for sub- and near-barrier fusion. Indeed, these effects were found in a number of complete fusion reactions leading to the formation of excited transuranium nuclei. For example, a significant difference of AD was observed at the center-of-mass energies below the Coulomb barrier in the $^{12}\text{C} + ^{235,236}\text{U}$ reactions [14,15]. It should be noted that the excitation energies of $^{247,248}\text{Cf}$ formed in the reactions were close to each other and exceeded 30 MeV. At such excitation energies, the specific features of fissioning nuclei (for example, shell effects in the fission barriers [16–18]) should not significantly affect AD. As is noted in Refs. [5,14,15], more significant factors are the deformations of the $^{236,235}\text{U}$ target nuclei and the nonzero spin in the ground state of the ^{235}U nucleus ($s_t = 7/2\hbar$) and its absence in ^{236}U . Indeed, because of the dependence of

*eremenko@sinp.msu.ru

the Coulomb barrier on the mutual orientation of the colliding deformed nuclei, both initial distributions over the total angular momentum (J) projections onto the symmetry axis (K) and the beam axis (M) for the nuclear system formed as a result of complete fusion will differ for these reactions at sub- and near-barrier energies. The observed ADs were interpreted as the manifestation of memory about the entrance channels of the reactions. For the above-barrier energies, the fusion probability loses the sensitivity to the mutual orientation of the deformed colliding nuclei and ADs become similar.

There is a dynamical model developed in Refs. [19–21] that is well suited for the consistent description of ADs in heavy-ion-induced reactions for a very wide energy range. Within this model, nuclear fission is described in a space of the deformation variable using the Langevin equations and the K value. K is considered as a variable undergoing random transitions throughout the evolution of the fissioning nucleus due to a coupling with the intrinsic degrees of freedom. The probabilities of such transitions for each phase of the fission process depend on the ratios between durations of these phases and the relaxation time for the tilting mode, τ_K . This model was successfully applied to describe the experimental data on ADA and prefission neutron multiplicities for a number of reactions leading to the formation of nuclei having such high angular momenta and temperatures that the concept of transition states at the saddle point of the fission barrier [2] becomes invalid. It should be also noted that the dynamic model contains both statistical models (the model of transition states in the saddle points of fission barriers [2] and the scission point model [22]) as special cases. For example, for nuclear fission with temperatures significantly lower than the fission barriers, the predictions of the dynamic and saddle point models are close. The analysis of experimental data on ADs performed with this model for a number of reactions with heavy ions showed that the relaxation time for the tilting mode was in the range $\tau_K = (20\text{--}30) \times 10^{-21}$ s. This value is close to fission times of heavy nuclei at temperatures comparable to the magnitudes of the fission barriers. In Ref. [23], the dynamical model was generalized to the case of the three-dimensional Langevin model. Now, the related approaches have been developed, in which the Langevin equation [24–26] has been used to describe the evolution of K . The main advantage of this model is a unified description of collective variables and K . However, K is defined in the discrete set consisting of $2J + 1$ values. Consequently, the approach used in Refs. [19–21] seems to be more justified for calculations at subbarrier energies, when small values of J play a significant role. On the other hand, it seems that both approaches are equally applicable and useful at above-barrier energies. Please note also that both models contain one adjustable parameter (τ_K or a dissipation coefficient for the tilting mode) and they are related to each other [25,26]. The advantage of the model in Refs. [19–21] is that it is free from assumptions about the magnitude of τ_K . Whereas in Refs. [24–26] the reduced Langevin equation is used to simulate the dynamics of K , which is justified only for large dissipation coefficients for the tilting mode (or short τ_K).

In this work, using the model in Refs. [19–21] as a basis, we develop a dynamic approach to analyze ADs for heavy-

ion-induced reactions, which takes into account the entrance channel effects, allows the analysis of experimental data in a wide energy range including subbarrier and high above-barrier energies, and provides new information on fusion and fission dynamics. It should be emphasized that the approaches of Refs. [9–11] are not appropriate for the analysis performed in this article. For example, the mass asymmetries of the entrance channels for the $^{12}\text{C} + ^{235,236}\text{U}$ reactions exceed the Businaro-Gallone value, while their ADA are very different for the sub-barrier energies (see Fig. 9). It is also expected that the quasifission contributions are vanishingly small [2] for these reactions. The pioneering and successful analysis of Refs. [14,15] was based on the standard transition-state model [2,8], modified for the rough accounting of the fission time scale. Moreover these studies were performed only for the near- and subbarrier energies with the use of the quasiclassical expression for the initial distribution of K .

II. CALCULATION OF THE INITIAL DISTRIBUTIONS OVER COMPONENTS OF THE TOTAL ANGULAR MOMENTUM

The effect of the entrance channel of a fusion reaction on the observed AD can be qualitatively clarified as follows. Let us first consider a simpler case of complete fusion of a spherically symmetric spinless particle with a deformed target nucleus. Here the height of the fusion barrier depends on the mutual orientation of the symmetry axis of the target nucleus and the momentum of the incident particle [27]. In other words, at beam energies close to (and below) the Coulomb barrier, fusion will occur predominantly with the tip of the deformed target nucleus. It should be emphasized that the spin s_t of the target nucleus in the ground state is oriented along the nucleus' symmetry axis [13]. Thus, in the case of collisions with a deformed target nucleus at subbarrier energies, fusion will predominantly occur for the s_t orientation along the incident particle momentum. Note that J of the system formed during fusion is the sum of the channel spin $S = s_t$ and the collisional orbital momentum ℓ , which in turn lies in the plane perpendicular to the beam (Fig. 1, left). Therefore, at subbarrier energies, the most probable values of K and M of the system formed will be 0 for target nuclei with $s_t = 0\hbar$ (Fig. 1, middle) and $K(M) = s_t$ when $s_t \neq 0\hbar$ (Fig. 1, right).

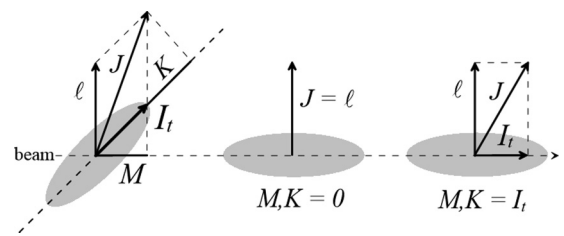


FIG. 1. Schematic diagram of the summation of angular momenta in the complete fusion reaction between a light nucleus and a heavy target nucleus having a nonzero spin in the ground state (left). The total angular momentum of the nuclear system produced in a subbarrier complete fusion for the most probable orientation of the target nuclei with $s_t = 0\hbar$ (middle) and $s_t \neq 0\hbar$ (right).

Obviously, with an increase of collision energy, the dependence of the fusion probability on the mutual orientation of the incident particle momentum and the deformed target nucleus will continuously weaken. When $s_t \neq 0\hbar$, at incident particle energies significantly exceeding the Coulomb barrier, different K and M should be occupied with almost equal probability and, therefore, the distributions over K and M should be equiprobable. Thus, the information about the partial fusion cross section at a certain orientation angle of a deformed target nucleus with respect to the beam axis makes it possible to derive the initial distributions over K and M for the fissioning system. For example, the following expression was obtained in Ref. [13] for the distribution over J and M :

$$Y(J, M) = \frac{\sum_{\ell=0}^{\infty} \sum_{\mu_t=-s_t}^{s_t} \sigma(\ell, \mu_t) |C_{\mu_t, 0, M}^{s_t, \ell, J}|^2}{\sum_{\ell=0}^{\infty} \sum_{\mu_t=-s_t}^{s_t} \sigma(\ell, \mu_t)}, \quad (1)$$

where μ_t is the component of s_t along the beam axis, $C_{\mu_t, 0, M}^{s_t, \ell, J}$ is the Clebsch-Gordan coefficient, and $\sigma(\ell, \mu_t)$ is the partial fusion cross section, which can be expressed in terms of the partial fusion cross sections dependent on the corresponding orientation angles as follows:

$$\sigma(\ell, \mu_t) = \int |d_{s_t, \mu_t}^{s_t}(\theta_t)|^2 \sigma(\ell, \theta_t) \sin(\theta_t) d\theta_t. \quad (2)$$

Here $d_{s_t, \mu_t}^{s_t}(\theta_t)$ is the symmetric-top wave function and θ_t is the orientation angle of the target nucleus with respect to the beam axis.

In this study, to calculate the initial distributions of the fissioning system over K , it is proposed to use the relations analogous to Eqs. (1) and (2):

$$Y(J, K) = \frac{\sum_{\ell=0}^{\infty} \sum_{K_\ell=-\ell}^{\ell} \sigma(\ell, K_\ell) |C_{s_t, K_\ell, K}^{s_t, \ell, J}|^2}{\sum_{\ell=0}^{\infty} \sum_{K_\ell=-\ell}^{\ell} \sigma(\ell, K_\ell)}, \quad (3)$$

where K_ℓ is the component of ℓ along the symmetry axis of the deformed target nucleus. The partial cross sections $\sigma(\ell, K_\ell)$ can be expressed in terms of the partial cross sections dependent on the corresponding orientation angles as follows:

$$\sigma(\ell, K_\ell) = \int |d_{K_\ell, 0}^{\ell}(\theta_t)|^2 \sigma(\ell, \theta_t) \sin(\theta_t) d\theta_t. \quad (4)$$

The expressions for $Y(J, M)$ and $Y(J, K)$ can easily be generalized to the case of a deformed incident particle with the spin s_p . To this end, it is necessary to take into account that $|s_t - s_p| \leq S \leq s_t + s_p$, while the maximum fusion probability of two nuclei at subbarrier energies corresponds to the tip-to-tip collisions. Then, $Y(J, M)$ can be written as

$$Y(J, M) = \sum_{\ell=0}^{\infty} \sum_{S=|s_t-s_p|}^{s_t+s_p} \sum_{\mu_t=-s_t}^{s_t} \sigma(\ell, \mu_t, M - \mu_t) \times \frac{|C_{M, 0, M}^{S, \ell, J}|^2 |C_{\mu_t, M - \mu_t, M}^{s_t, s_p, S}|^2}{\sum_{\ell=0}^{\infty} \sum_{\mu_t=-s_t}^{s_t} \sum_{\mu_p=-s_p}^{s_p} \sigma(\ell, \mu_t, \mu_p)}, \quad (5)$$

where

$$\sigma(\ell, \mu_t, \mu_p) = \iint |d_{s_t, \mu_t}^{s_t}(\theta_t)|^2 |d_{s_p, \mu_p}^{s_p}(\theta_p)|^2 \times \sigma(\ell, \theta_t, \theta_p) \sin(\theta_t) \sin(\theta_p) d\theta_t d\theta_p. \quad (6)$$

In expressions (5) and (6), μ_p is the component of s_p along the beam axis and θ_p is the corresponding orientation angle. In calculation of $Y(J, K)$, it is necessary to take into account that K is the sum of the components of three vectors (ℓ , s_t , and s_p) along the symmetry axis of the deformed target nucleus:

$$Y(J, K) = \sum_{\ell=0}^{\infty} \sum_{S=|s_t-s_p|}^{s_t+s_p} \sum_{K_\ell=-\ell}^{\ell} \sigma(\ell, K_\ell, K_p) \times \frac{|C_{K-K_\ell, K_\ell, K}^{S, \ell, J}|^2 |C_{s_t, K-s_t-K_\ell, K-K_\ell}^{s_t, s_p, S}|^2}{\sum_{\ell=0}^{\infty} \sum_{K_\ell=-\ell}^{\ell} \sum_{K_p=-s_p}^{s_p} \sigma(\ell, K_\ell, K_p)}, \quad (7)$$

and

$$\sigma(\ell, K_\ell, K_p) = \iint |d_{K_\ell, 0}^{\ell}(\theta_t)|^2 |d_{s_p, K_p}^{s_p}(\theta_p)|^2 \times \sigma(\ell, \theta_t, \theta_p) \sin(\theta_t) \sin(\theta_p) d\theta_t d\theta_p. \quad (8)$$

Here K_p is the component of the vector s_p along the symmetry axis of the deformed target nucleus.

III. CALCULATION OF THE FUSION CROSS SECTIONS FOR TARGET NUCLEI AND INITIAL DISTRIBUTIONS OVER K AND M

In this study, the fusion cross sections were calculated on the assumption of collisions of spherical incident nuclei with deformed target nuclei, which is quite justified for the $^{12,13}\text{C} + ^{235,236,238}\text{U}$ and $^{16}\text{O} + ^{232}\text{Th}$ reactions under study.

The nucleus-nucleus potential was calculated as a sum of the nuclear, Coulomb, and rotational energies: $V = V_N + V_C + V_{\text{rot}}$. For the nuclear part of the interaction potential, we used the Woods-Saxon potential

$$V_N = \frac{-V_0}{1 + \exp\left(\frac{R - R_p(\theta_p) - R_t(\theta_t)}{a}\right)}. \quad (9)$$

Here R is the distance between the centers of mass of the colliding nuclei, V_0 is the potential depth, a is the diffusivity parameter, and $R_{p,t}$ are the radii of the incident and target nuclei, which were assumed to be

$$R_{p,t} = r_0 A^{1/3} (1 + \beta_{p,t} Y_{20}(\theta_{p,t})). \quad (10)$$

For the Coulomb part of the potential, we used the expressions obtained in Ref. [28], in which only the terms related to quadrupole deformation of the target nucleus were left. The rotational term of the nucleus-nucleus potential was calculated as

$$V_{\text{rot}} = \frac{\hbar^2 \ell(\ell + 1)}{2mR^2}, \quad (11)$$

where m is the reduced mass of the colliding nuclei. The partial fusion cross section was determined as

$$\sigma(\ell, \theta_p, \theta_t) = \frac{\pi \hbar^2}{2\mu E_{\text{c.m.}}} \frac{2\ell + 1}{1 + \exp\left(\frac{2\pi[B(\ell, \theta_t, \theta_p) - E_{\text{c.m.}}]}{\hbar\omega(\ell, \theta_t, \theta_p)}\right)}, \quad (12)$$

where $B(\ell, \theta_t, \theta_p)$ is the Coulomb barrier and $\hbar\omega(\ell, \theta_t, \theta_p)$ is the oscillator frequency of the potential near its maximum.

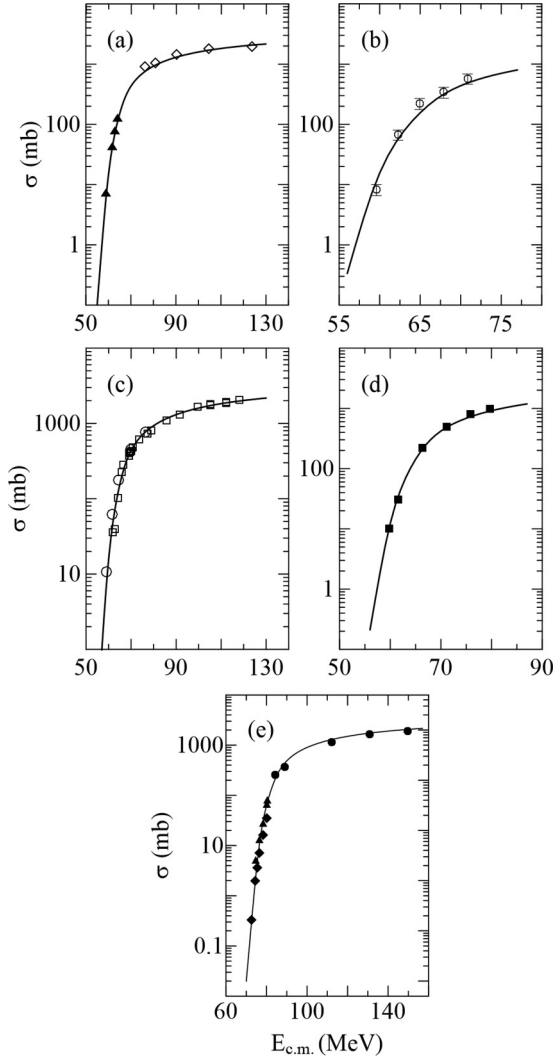


FIG. 2. Fission cross sections as functions of $E_{c.m.}$ for the $^{12}\text{C} + ^{236}\text{U}$ (a), $^{12}\text{C} + ^{235}\text{U}$ (b), $^{12}\text{C} + ^{238}\text{U}$ (c), $^{13}\text{C} + ^{235}\text{U}$ (d), and $^{16}\text{O} + ^{232}\text{Th}$ (e) reactions. Experimental data are represented by points: \blacktriangle are taken from Ref. [31], \diamond from Ref. [32], \circ from Ref. [14], \square from Ref. [33], \blacksquare from Ref. [34], \bullet from Ref. [4], and \blacklozenge from Ref. [35]. The curves are the model calculations (see text).

The total fusion cross section was calculated by the formula

$$\sigma_f = \sum_{\ell=0}^{\infty} \iint \sigma(\ell, \theta_t, \theta_p) \sin(\theta_t) \sin(\theta_p) d\theta_t d\theta_p. \quad (13)$$

In analysis of the experimental data on the fusion cross sections for the $^{12,13}\text{C} + ^{235,236,238}\text{U}$ and $^{16}\text{O} + ^{232}\text{Th}$ reactions, only the a and r_0 parameters were varied. The potential depth was fixed and its value was chosen to be the same as that in Ref. [29], $V_0 = 70$ MeV. The quadrupole deformation parameters for the target nuclei were taken from Ref. [30]: $\beta = 0.207$ and 0.215 for ^{232}Th and $^{235,236,238}\text{U}$, respectively. In Fig. 2, the results of calculations of the complete fusion cross sections are compared with the experimental data. The following diffusivities are obtained: $a = 0.50$ fm for all reactions. The r_0 parameter was chosen to be 1.23 fm

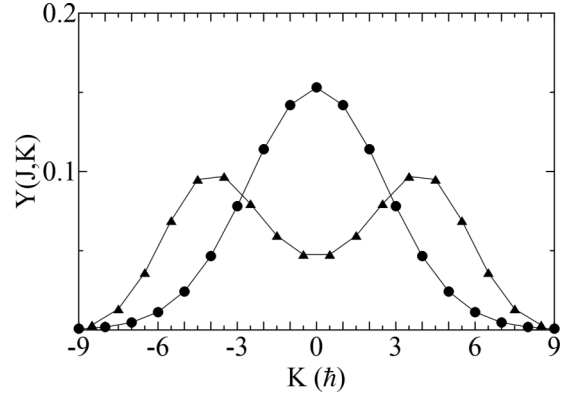


FIG. 3. Initial distributions over K at the subbarrier energy $E_{c.m.} = 55$ MeV. The calculations are presented for ^{247}Cf produced with $J = 17/2\hbar$ in the $^{12}\text{C} + ^{235}\text{U}$ reaction (\blacktriangle) and for ^{248}Cf produced with $J = 9\hbar$ in the $^{12}\text{C} + ^{236}\text{U}$ reaction (\bullet).

for the $^{12,13}\text{C} + ^{235,236,238}\text{U}$ reactions and 1.245 fm for the $^{16}\text{O} + ^{232}\text{Th}$ reaction.

Thus, the determined cross sections $\sigma(\ell, \theta_t, \theta_p)$ were used in the calculations of the initial distributions over J , K , and M according to relations (5)–(8). In Fig. 3, the initial distributions over K are compared for the $^{12}\text{C} + ^{235}\text{U}$ and ^{236}U reactions for the subbarrier energy $E_{c.m.} = 55$ MeV. The fusion barriers are in the range 56–65 MeV for the $^{12,13}\text{C} + ^{235,236,238}\text{U}$ reactions and 73–84 MeV for the $^{16}\text{O} + ^{232}\text{Th}$ reaction dependent on the mutual orientation of the colliding nuclei. It can be seen that the distribution $Y(J, K)$ has two maxima near $K = \pm 7/2\hbar$ for the $^{12}\text{C} + ^{235}\text{U}$ reaction. The positions of the maxima correspond to two possible components of s_t along the symmetry axis of the deformed target nucleus ^{235}U . In addition, these data show that the existence of the nonzero spin of the target nucleus results in a much wider initial distribution over K for the $^{12}\text{C} + ^{235}\text{U}$ reaction, and this circumstance should result in lower ADA at subbarrier energies in this case. Broadening of the distributions over K with an increase in the incident particle energy is shown in Figs. 4 and 5. Such behavior of $Y(J, K)$ is due to the gradual decrease of

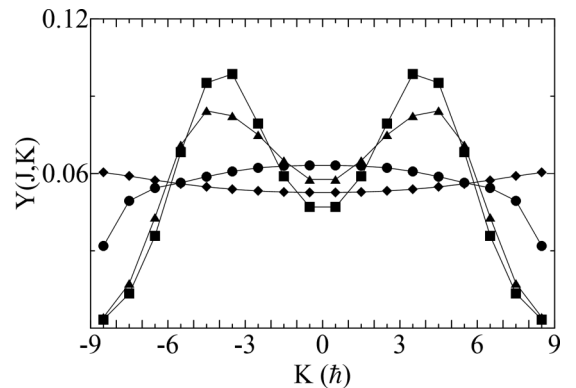


FIG. 4. Initial distributions over K for ^{247}Cf produced with $J = 17/2\hbar$ in the $^{12}\text{C} + ^{235}\text{U}$ reaction at $E_{c.m.} = 55$ (\blacksquare), 60 (\blacktriangle), 65 (\bullet), and 70 (\blacklozenge) MeV.

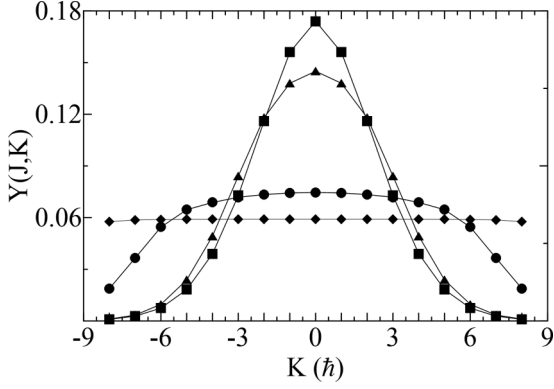


FIG. 5. Initial distributions over K for ^{248}Cf produced with $J = 8\hbar$ in the $^{12}\text{C} + ^{236}\text{U}$ reaction at $E_{\text{c.m.}} = 55$ (■), 60 (▲), 65 (●), and 70 (◆) MeV.

the sensitivity of the fusion probability to the target nucleus orientation at energies above the fusion barrier.

Finally, Fig. 6 shows the results of calculations of the initial distributions over M for the $^{12}\text{C} + ^{235}\text{U}$ reaction at four energies of incident carbon ions. As was expected, $Y(J, M)$ has two pronounced peaks at $M = \pm 7/2\hbar$ at subbarrier energies and becomes equiprobable for above-barrier energies.

IV. ANALYSIS OF ANGULAR DISTRIBUTIONS OF FISSION FRAGMENTS WITHIN THE DYNAMIC MODEL

In this study, ADs were calculated using the dynamic model proposed in Refs. [19–21]. Within this model, the induced fission dynamics is described using a system of stochastic Langevin equations for one collective coordinate r and the corresponding momentum p :

$$\begin{aligned} \frac{dr}{dt} &= \frac{p}{m(r)} \\ \frac{dp}{dt} &= -\frac{1}{2} \frac{d}{dr} \left(\frac{p^2}{m(r)} \right) - \frac{dF}{dr} - \beta(r)p + f(t). \end{aligned} \quad (14)$$

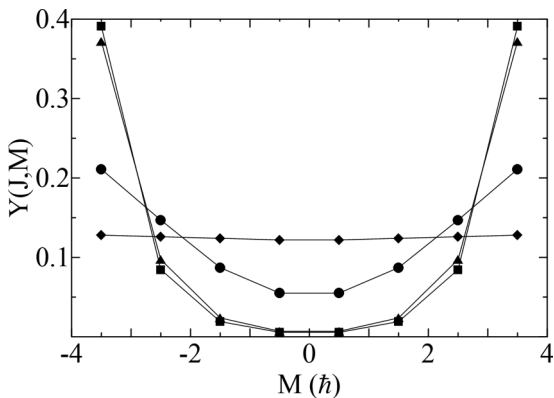


FIG. 6. Initial distributions over M for ^{247}Cf produced in the $^{12}\text{C} + ^{235}\text{U}$ reaction at $E_{\text{c.m.}} = 55$ (■), 60 (▲), 65 (●), and 70 (◆) MeV.

Here r is the distance between the centers of mass of the two halves of the nucleus along the fission valley. The fission valley is determined by the method proposed in Ref. [36] using the parametrization of Ref. [37] for axially and mirror symmetrical nuclear shapes. In Eq. (14) $\beta(r)$ is the damping parameter of the fission mode, and f is a random force with the following properties: $\langle f(t) \rangle = 0$ and $\langle f(t_1), f(t_2) \rangle = 2D(r)\delta(t_1 - t_2)$. $D(r)$ is assumed to satisfy the Einstein relation $D(r) = m(r)\beta(r)T$, where T is the nuclear temperature. The inertial parameter $m(r)$ was calculated along the fission valley using the hydrodynamic Werner-Wheeler approximation [38] and the method described in Ref. [39]. The conservative forces in Eq. (14) were determined as a derivative of the free energy $F(r, T, J, K) = V(r, J, K) - a_d(r)T^2$. In this case, it was assumed that the nuclear temperature obeys the relation $T = \sqrt{E_{\text{int}}/a_d(r)}$, with $E_{\text{int}} = E^* - p^2/(2m) - V(r, J, K)$, where E^* is the total nucleus excitation energy. The parameter of level density a_d was assumed to be dependent on deformation: $a_d(r) = a_{1d}A + a_{2d}A^{2/3}B_S(r)$, where A is the mass number of the fissioning nucleus and $B_S(r)$ is the dimensionless surface energy functional. The values of a_{1d} and a_{2d} were taken from Ref. [40]. In calculation of the potential energy of the rotating nuclear system, its dependence on K was taken into account:

$$\begin{aligned} V(r, J, K) &= B_S(r)E_S^0(Z, A) + B_C(r)E_C^0(Z, A) \\ &+ \frac{[J(J+1) - K]^2\hbar^2}{2\mathfrak{I}_\perp} + \frac{K^2\hbar^2}{2\mathfrak{I}_\parallel}, \end{aligned} \quad (15)$$

here Z is the charge of the fissioning nucleus; $B_C(r)$ is a dimensionless Coulomb energy functional; E_S^0 and E_C^0 are the surface and Coulomb energies of the corresponding spherical system, respectively; and \mathfrak{I}_\perp and \mathfrak{I}_\parallel are the momenta of inertia with respect to the axes perpendicular and parallel to the symmetry axis of the fissioning nucleus. The approximations suggested in Ref. [36] were used to calculate both $B_S(r)$ and $B_C(r)$.

To take into account the evaporation of light precession particles (neutrons, protons, α particles, and γ quanta), calculations of the corresponding decay probabilities for an excited system within the statistical theory of nuclear reactions were incorporated into dynamic calculations. The algorithm of such calculations is described in detail in Refs. [6,23,41]. The initial values of r and p were generated for each Langevin sample, proceeding from the distribution in the form

$$\Phi(r, p, J) = \frac{1}{\sqrt{2\pi mT}} \exp\left(-\frac{p^2}{2mT}\right) \delta(r - r_{\text{eq}}). \quad (16)$$

Here r_{eq} is the collective coordinate for the equilibrium deformation. The initial values of J , K , and M were generated from the distributions $Y(J, K)$ and $Y(J, M)$, taking into account only discrete values within the ranges $-J \leq K \leq J$ and $-S \leq M \leq S$.

Within the dynamic model, K was considered to be fluctuating due to the interaction with the intrinsic degrees of freedom. The algorithm of calculations taking into account fluctuations of K is as follows. At each step of the numerical integration of the system of stochastic Langevin equations (14), the probability of changing K is considered. This

probability is assumed to be equal to h/τ_K , where h is the numerical integration step for the Langevin equations. Furthermore, a random number, ξ , is generated, which has a uniform distribution on the interval $[0,1]$. If the condition $\xi < h/\tau_K$ is satisfied, a new value is assigned to K , which is chosen from the distribution

$$P(K) \propto \exp\left(-\frac{\Delta F(r, J, K, T)}{T}\right). \quad (17)$$

Here ΔF is the free energy variation with the change of K . Other details of the dynamic model are described in Refs. [19,21]. Thus, within the approach proposed, each Langevin sample reaching the scission point is characterized by certain values of J , K , and M . It should be emphasized that J at the scission point differs from the initial value due to emission of the light particles. Accordingly, the values of K were corrected after each emission event. In addition, we neglected the variation in M as a result of emission of light particles. This assumption is quite justified and often used for reactions induced by heavy ions [3,4,19,21,23,25,26]. As a result, ADs are calculated as an average over the ensemble of Langevin samples leading to fission:

$$W(\theta) = \frac{1}{N_f} \sum_{i=1}^{N_f} \frac{1}{2} (2J_i + 1) |d_{K_i, M_i}^{J_i}(\theta)|^2, \quad (18)$$

where N_f is the number of Langevin samples reaching the scission point.

Within this approach, ADs depend strongly on the relationship between the relaxation time τ_K and the durations of different stages of fission. Thus, it is necessary to determine with maximum accuracy the time scale of induced fission and, therefore, the damping coefficient β of the collective nuclear motion. To calculate β , we used the one-body mechanism of nuclear dissipation [42] (wall + window formula [43–45]). As a free parameter, we introduced the reduction coefficient k_s , which makes it possible to decrease the contribution to dissipation from the interaction of nucleons with the nucleus surface

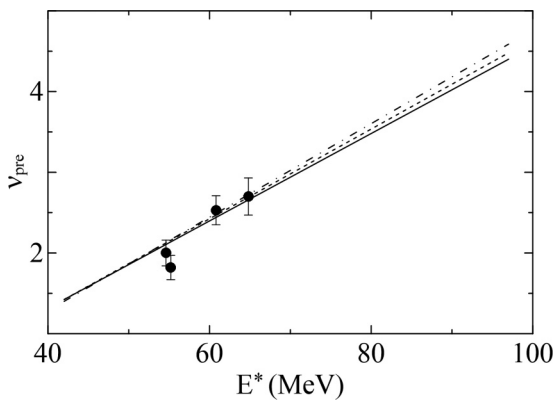


FIG. 7. Multiplicity of pre-scission neutrons (v_{pre}). Experimental data for the $^{16}\text{O} + ^{232}\text{Th}$ reaction are taken from Ref. [46]. The calculation results are presented for the reaction leading to production of the ^{248}Cf compound nuclei: the solid line is for the $^{16}\text{O} + ^{232}\text{Th}$ reaction, the dashed line for the $^{12}\text{C} + ^{236}\text{U}$ reaction, and the dashed-dotted line for the $^{13}\text{C} + ^{235}\text{U}$ reaction.

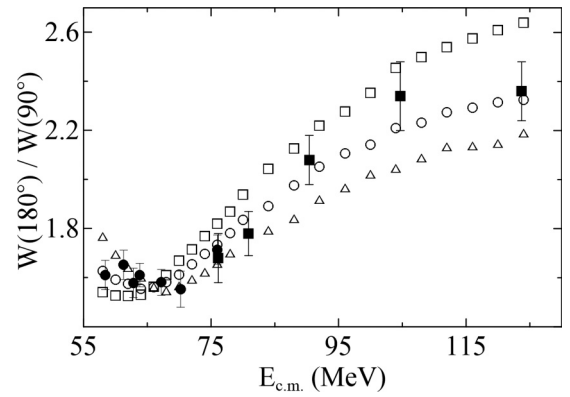


FIG. 8. Comparison of ADA calculation with different $\tau_K = 10 \times 10^{-21}$ s (\square), 20×10^{-21} s (\circ), and 30×10^{-21} s (\triangle) and the experimental data for the $^{12}\text{C} + ^{236}\text{U}$ reaction (\bullet , Refs. [14,15]; \blacksquare , Ref. [32]).

[43]. To determine the k_s value, we used the experimental data on the multiplicity of pre-scission neutrons. It should be noted that the multiplicity of light pre-scission particles is almost independent of τ_K [19–21,23,25,26]. This circumstance allows one to determine the coefficient k_s on the basis of analysis of neutron multiplicities and then varying τ_K to describe the experimental ADA. Note that, among the $^{12}\text{C} + ^{235,236,238}\text{U}$ and $^{16}\text{O} + ^{232}\text{Th}$ reactions under consideration, only the latter one is characterized by experimental data on the multiplicity of pre-scission neutrons [46]. However, the $^{12}\text{C} + ^{236}\text{U}$ and $^{13}\text{C} + ^{235}\text{U}$ reactions also lead to the formation of ^{248}Cf and, as it was shown in Ref. [2], the observed average multiplicity of pre-scission neutrons depends strongly only on Z/A and the excitation energy of the fissioning system. In Fig. 7, the experimental data on the multiplicity of pre-scission neutrons for the $^{16}\text{O} + ^{232}\text{Th}$ reaction are compared with the results of calculations. In this case, proceeding from the requirement of the best description of the experimental data, we estimated $k_s = 0.2$.

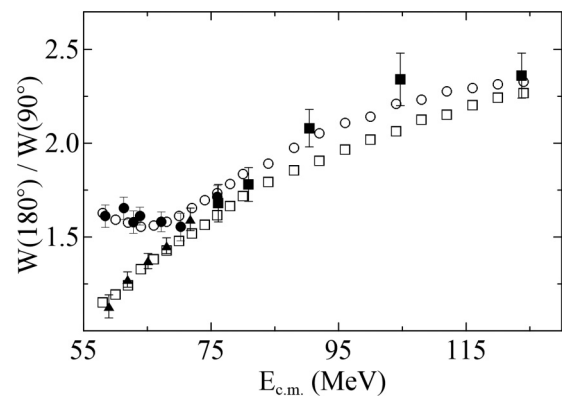


FIG. 9. Comparison of the experimental ADA and the calculations performed with $\tau_K = 20 \times 10^{-21}$ s. For the $^{12}\text{C} + ^{236}\text{U}$ reaction the experimental points are marked as in Fig. 8, the calculation results are presented by \circ . For the $^{12}\text{C} + ^{235}\text{U}$ reaction, the experimental points [14,15] are marked as \blacktriangle , and the calculation results are presented by \square .

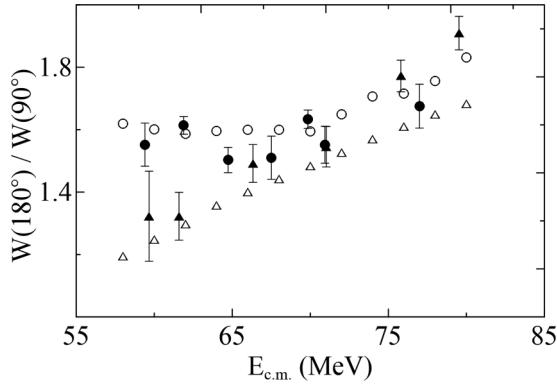


FIG. 10. The same as in Fig. 9. For the $^{12}\text{C} + ^{238}\text{U}$ reaction the experimental points [14,15] are marked as ●, and the calculation results are marked as ○. For the $^{13}\text{C} + ^{235}\text{U}$ reaction, the experimental points [34] are marked as ▲, and the calculation results are marked as △.

Selected in this way k_s was used to calculate ADs. Further, we varied only τ_K to achieve the best description of the experimental data on ADs with the use of the initial distributions (5)–(8). Figure 8 shows the sensitivity of the ADA calculations to the choice of the τ_K value. As can be seen, for the subbarrier energies an increase of τ_K leads to the increase of ADA. This is due to the increasing role of fission occurring in time not exceeding τ_K . In contrast, the decrease of ADA for the above-barrier energies with the τ_K rise indicates the increasing role of configurations more distant from the scission point. The best description of the experimental ADA in the whole energy range under study provides the $\tau_K = 20 \times 10^{-21}$ s value. It should be noted that this value falls within the τ_K range from Refs. [19–21] where the experimental ADA were analyzed for a number of reactions in the framework of the dynamical model only for the above-barrier energies. Figures 9 and 10 demonstrate the quality of the description of experimental ADA with $\tau_K = 20 \times 10^{-21}$ s and $k_s = 0.2$ for all reactions under study. These results suggest the following statement. For the energies of incident particles below the Coulomb barrier, ADs are significantly influenced by the

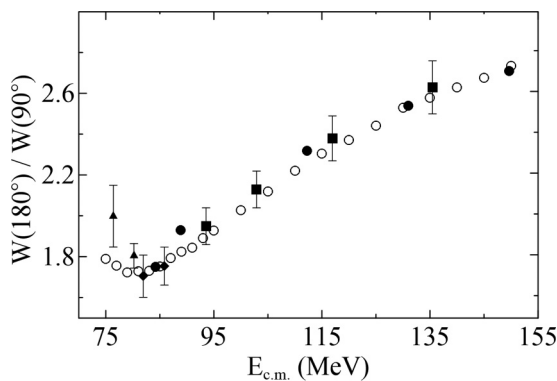


FIG. 11. The same as in Fig. 9 for the $^{16}\text{O} + ^{232}\text{Th}$ reaction. Experimental points are marked as follows: ●, from Ref. [4]; ■, from Ref. [32]; ◆, from Ref. [9]; and ▲, from Ref. [47]. The calculation results are presented as ○.

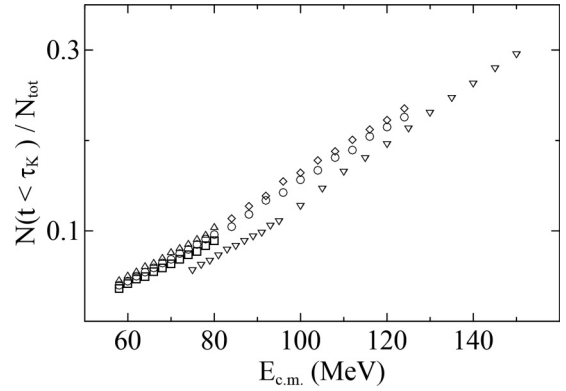


FIG. 12. The fraction of fission events occurring in a time not exceeding τ_K in the total yield of fission fragments for the $^{12}\text{C} + ^{236}\text{U}$ (○), $^{12}\text{C} + ^{235}\text{U}$ (◇), $^{12}\text{C} + ^{238}\text{U}$ (□), $^{13}\text{C} + ^{235}\text{U}$ (△), and $^{16}\text{O} + ^{232}\text{Th}$ (▽) reactions. For the $^{12}\text{C} + ^{235}\text{U}$ reaction the calculation results are not presented in the range $E_{c.m.} = 58\text{--}84$ MeV due to the overlap with the results for the $^{12}\text{C} + ^{236}\text{U}$ and $^{13}\text{C} + ^{235}\text{U}$ reactions.

memory of the reaction entrance channels. For this reason both in the calculations and in the experimental data there are significant differences of ADA for the reactions on the ^{235}U target nuclei with the nonzero ground-state spin and the spinless $^{238,236}\text{U}$ target nuclei. For the above-barrier energies, when the initial distributions over K and M tend to be equiprobable, the magnitudes and the energy dependencies of ADA become similar. Changing behavior of ADA in the transition from the sub- to above-barrier energies is also observed both in the calculations and in the experimental data for the $^{16}\text{O} + ^{232}\text{Th}$ reaction (Fig. 11). Here the discrepancy between the calculations and the experimental data at the subbarrier energies can be explained by the contribution of quasifission [48].

Thus, the developed dynamic approach allows the analysis of experimental data on ADs of excited heavy nuclei produced in heavy-ion-induced reactions in a wide energy range, including the subbarrier energies, where the memory effects play an important role, and above-barrier energies, where the existing statistical models are not applicable. This approach allows us to study the phenomenon of nuclear dissipation, the complete fusion processes, and to obtain information about the induced fission time scale. In particular, in this work we have identified the contribution of fission events occurring in time shorter than τ_K in the total fragment yields (Fig. 12). As can be seen from Fig. 12 the fraction of such events in the subbarrier range is not more than 0.1 for all reactions under study. Here it should be noted that these results may change, considering the dependencies of τ_K on the deformation, the angular momentum, and perhaps the temperature. In the future, using such dependencies we plan to analyze the available data [26,49,50] on these dependencies using not only AD but also other fission characteristics (e.g., fragment spins).

V. CONCLUSIONS

A dynamic approach suitable for the analysis of ADs for complete fusion-fission reactions with heavy ions has been

developed. This approach is applicable to a wide energy range starting from subbarrier fusion and ending with the collision energies when the fission at temperatures higher than fission barrier values plays an important role. On the basis of the results of Ref. [13] we suggested the quantum-mechanical expressions to calculate the initial distributions over K . The

experimental data analysis on ADA and precision neutron multiplicities for a number of reactions leading to the production of the Cf isotopes has provided the information on nuclear viscosity, the relaxation time of the tilting mode, and the fraction of fission events occurring before the establishment of the equilibrium distribution over K .

-
- [1] S. Kailas, *Phys. Rep.* **284**, 381 (1997).
- [2] J. O. Newton, *Fiz. Elem. Chastits At. Yadra* **21**, 821 (1990) [*Sov. J. Part. Nucl.* **21**, 349 (1990)].
- [3] B. B. Back, *Phys. Rev. C* **31**, 2104 (1985).
- [4] B. B. Back, R. R. Betts, J. E. Gindler, B. D. Wilkins, S. Saini, M. B. Tsang, C. K. Gelbke, W. G. Lynch, M. A. McMahan, and P. A. Baisden, *Phys. Rev. C* **32**, 195 (1985).
- [5] R. G. Thomas, R. K. Choudhury, A. K. Mohanty, A. Saxena, and S. S. Kapoor, *Phys. Rev. C* **67**, 041601(R) (2003).
- [6] V. A. Drozdov, D. O. Eremenko, S. Yu. Platonov, O. V. Fotina, and O. A. Yuminov, *Yad. Fiz.* **64**, 221 (2001) [*Phys. Atom. Nucl.* **64**, 179 (2001)].
- [7] V. A. Drozdov, D. O. Eremenko, O. V. Fotina, S. Yu. Platonov, O. A. Yuminov, and G. Giardina, *Yad. Fiz.* **66**, 1669 (2003) [*Phys. Atom. Nucl.* **66**, 1622 (2003)].
- [8] R. Vandenbosch and J. R. Huizenga, *Nuclear Fission* (Academic Press, New York, 1973).
- [9] V. S. Ramamurthy, S. S. Kapoor, R. K. Choudhury, A. Saxena, D. M. Nadkarni, A. K. Mohanty, B. K. Nayak, S. V. Sastry, S. Kailas, A. Chatterjee, P. Singh, and A. Navin, *Phys. Rev. Lett.* **65**, 25 (1990).
- [10] Z. Liu, H. Zhang, J. Xu, Y. Qiao, X. Qian, and C. Lin, *Phys. Rev. C* **54**, 761 (1996).
- [11] D. J. Hinde, M. Dasgupta, J. R. Leigh, J. P. Lestone, J. C. Mein, C. R. Morton, J. O. Newton, and H. Timmers, *Phys. Rev. Lett.* **74**, 1295 (1995).
- [12] D. J. Hinde, M. Dasgupta, J. R. Leigh, J. C. Mein, C. R. Morton, J. O. Newton, and H. Timmers, *Phys. Rev. C* **53**, 1290 (1996).
- [13] R. D. Butt, M. Dasgupta, I. Gontchar, D. J. Hinde, A. Mukherjee, A. C. Berriman, C. R. Morton, J. O. Newton, A. E. Stuchbery, and J. P. Lestone, *Phys. Rev. C* **65**, 044606 (2002).
- [14] J. P. Lestone, A. A. Sonzogni, M. P. Kelly, and R. Vandenbosch, *Phys. Rev. C* **56**, R2907(R) (1997).
- [15] J. P. Lestone, A. A. Sonzogni, M. P. Kelly, and R. Vandenbosch, *J. Phys. G: Nucl. Part. Phys.* **23**, 1349 (1997).
- [16] V. A. Drozdov, D. O. Eremenko, S. Yu. Platonov, O. V. Fotina, O. A. Yuminov, G. Mandaglio, F. Manganaro, and V. M. Romaniuk, *Int. J. Mod. Phys. E* **19**, 1249 (2010).
- [17] V. A. Drozdov, D. O. Eremenko, S. Yu. Platonov, O. V. Fotina, O. A. Yuminov, G. Giardina, G. Fazio, F. Malaguti, P. Oliva, and V. Togo, *Int. J. Mod. Phys. E* **19**, 1227 (2010).
- [18] D. O. Eremenko, B. Mellado, S. Yu. Platonov, O. V. Fotina, O. A. Yuminov, G. Giardina, G. Rappazzo, and F. Malaguti, *J. Phys. G: Nucl. Part. Phys.* **22**, 1077 (1996).
- [19] V. A. Drozdov, D. O. Eremenko, O. V. Fotina, S. Yu. Platonov, and O. A. Yuminov, *AIP Conf. Proc.* **704**, 130 (2004).
- [20] V. A. Drozdov, D. O. Eremenko, O. V. Fotina, S. Yu. Platonov, G. Giardina, F. Malaguti, and O. A. Yuminov, *Nucl. Phys. A* **734**, 225 (2004).
- [21] D. O. Eremenko, V. A. Drozdov, M. H. Eslamizadex, S. Yu. Platonov, O. V. Fotina, and O. A. Yuminov, *Phys. At. Nucl.* **69**, 1423 (2006).
- [22] P. D. Bond, *Phys. Rev. C* **32**, 471 (1985).
- [23] A. V. Karpov, R. M. Hiryanov, A. V. Sagdeev, and G. D. Adeev, *J. Phys. G: Nucl. Part. Phys.* **34**, 255 (2007).
- [24] J. P. Lestone, *Phys. Rev. C* **59**, 1540 (1999).
- [25] P. N. Nadtochy, E. G. Ryabov, A. E. Gegechkori, Yu. A. Anischenko, and G. D. Adeev, *Phys. Rev. C* **85**, 064619 (2012).
- [26] P. N. Nadtochy, E. G. Ryabov, A. E. Gegechkori, Yu. A. Anischenko, and G. D. Adeev, *Phys. Rev. C* **89**, 014616 (2014).
- [27] I. I. Gontchar, M. Dasgupta, D. J. Hinde, R. D. Butt, and A. Mukherjee, *Phys. Rev. C* **65**, 034610 (2002).
- [28] N. Takigawa, T. Rumin, and N. Ihara, *Phys. Rev. C* **61**, 044607 (2000).
- [29] A. S. Il'inov, Yu. Ts. Oganessian, and E. A. Cherepanov, *Sov. J. Nucl. Phys.* **36**, 69 (1982).
- [30] P. Moller, J. R. Nix, W. D. Myers, and W. J. Swiatecki, *At. Data Nucl. Data Tables* **59**, 185 (1995).
- [31] T. Murakami, C.-C. Sahm, R. Vandenbosch, D. D. Leach, A. Ray, and M. J. Murphy, *Phys. Rev. C* **34**, 1353 (1986).
- [32] S. Kailas, D. M. Nadkarni, A. Chatterjee, A. Saxena, S. S. Kapoor, R. Vandenbosch, J. P. Lestone, J. F. Liang, D. J. Prindle, A. A. Sonzogni, and J. D. Bierman, *Phys. Rev. C* **59**, 2580 (1999).
- [33] V. E. Viola and T. Sikkland, *Phys. Rev.* **128**, 767 (1962).
- [34] B. P. Ajitkumar, K. M. Varier, B. V. John, A. Saxena, B. K. Nayak, D. C. Biswas, R. G. Thomas, and S. Kailas, *Phys. Rev. C* **77**, 021601(R) (2008).
- [35] H. Zhang, Z. Liu, J. Xu, X. Qian, Y. Qiao, C. Lin, and K. Xu, *Phys. Rev. C* **49**, 926 (1994).
- [36] J. P. Lestone, *Phys. Rev. C* **51**, 580 (1995).
- [37] S. Trentalange, S. E. Koonin, and A. J. Sierk, *Phys. Rev. C* **22**, 1159 (1980).
- [38] K. T. R. Davies, A. J. Sierk, and J. R. Nix, *Phys. Rev. C* **13**, 2385 (1976).
- [39] J. Bartel, K. Mahboub, J. Richert, and K. Pomorski, *Z. Phys. A* **354**, 59 (1996).
- [40] A. V. Ignatyuk, M. G. Itkis, V. N. Okolovich, G. N. Smirenkin, and A. S. Tishin, *Yad. Fiz.* **21**, 1185 (1975) [*Sov. J. Nucl. Phys.* **21**, 612 (1975)].
- [41] P. Fröbrich and I. I. Gontchar, *Phys. Rep.* **292**, 131 (1998).
- [42] J. Blocki, Y. Bohen, J. R. Nix, J. Randrup, M. Robel, A. J. Sierk, and W. J. Swiatecki, *Ann. Phys. (New York)* **113**, 330 (1978).
- [43] J. R. Nix and A. G. Sierk, in *Proceedings of the International School-Seminar on Heavy Ion Physics, Dubna, 23–30 September 1986* (JINR, Dubna, 1987), p. 453.
- [44] A. J. Sierk and J. R. Nix, *Phys. Rev. C* **21**, 982 (1980).

- [45] G. D. Adeev, A. V. Karpov, P. N. Nadtochi, and D. V. Vanin, *Fiz. Elem. Chastits At. Yadra* **36**, 732 (2005) [*Phys. Part. Nucl.* **36**, 378 (2005)].
- [46] A. Saxena, A. Chatterjee, R. K. Choudhury, S. S. Kapoor, and D. M. Nadkarni, *Phys. Rev. C* **49**, 932 (1994).
- [47] R. Vandenbosch, T. Murakami, C.-C. Sahm, D. D. Leach, A. Ray, and M. J. Murphy, *Phys. Rev. Lett.* **56**, 1234 (1986).
- [48] N. Majumdar, P. Bhattacharya, D. C. Biswas, R. K. Choudhury, D. M. Nadkarni, and A. Saxena, *Phys. Rev. C* **53**, R544(R) (1996).
- [49] V. A. Drozdov, D. O. Eremenko, O. V. Fotina, S. Yu. Platonov, O. A. Yuminov, G. Mandaglio, M. Manganaro, and G. Fazio, *Int. J. Mod. Phys. E* **19**, 1125 (2010).
- [50] J. P. Lestone and S. G. McCalla, *Phys. Rev. C* **79**, 044611 (2009).